Oncology Research, Vol. 28, pp. 299–309
Printed in the USA.

0965-0407/20 $90.00 + .00
https://doi.org/10.3727/096504020X15796890809840
E-ISSN 1555-3906
www.cognizantcommunication.com

MafF Is Regulated via the circ-ITCH/miR-224-5p Axis and Acts as a Tumor Suppressor in Hepatocellular Carcinoma

Minhua Wu,*[1] Xubin Deng,†[1] Yu Zhong,‡[1] Li Hu,* Xiujuan Zhang,§ Yanqin Liang,* Xiaofang Li,¶ and Xiaoxia Ye*

*Department of Histology and Embryology, Guangdong Medical University, Zhanjiang, P.R. China
†Affiliated Cancer Hospital & Institute of Guangzhou Medical University, Guangzhou, P.R. China
‡Analysis Center, Guangdong Medical University, Zhanjiang, P.R. China
§Department of Physiology, Guangdong Medical University, Zhanjiang, P.R. China
¶Pathological Diagnosis and Research Center, Affiliated Hospital of Guangdong Medical University, Zhanjiang, P.R. China

MafF is a member of the basic leucine zipper (bZIP) transcription factor Maf family and is commonly downregulated in multiple cancers. But the expression and function of MafF in hepatocellular carcinoma (HCC) remain unclear. In this study, we investigated the relationship between endogenous MafF expression and HCC progression and explored the regulatory mechanism of MafF expression in HCC. We found that MafF decreased in HCC tissues and cells. Lentivirus-mediated MafF overexpression inhibited HCC cell proliferation and induced cell apoptosis. Bioinformatics analysis and luciferase assay identified MafF as a direct target of miR-224-5p. RNA pull-down assay demonstrated that circular RNA circ-ITCH could sponge miR-224-5p specifically in HCC. The rescue experiments further elucidated that the expression and antitumor effects of MafF could be regulated via the circ-ITCH/miR-224-5p axis. This study verified that MafF acted as a tumor suppressor in HCC and revealed the upstream regulation mechanism of MafF, which provided a new perspective for potential therapeutic targets of HCC.

Key words: MafF; miR-224-5p; circ-ITCH; Hepatocellular carcinoma (HCC)

INTRODUCTION

Hepatocellular carcinoma (HCC) is the sixth most common cancer in the world and the second cause of cancer-related mortality[1,2]. Clinically, HCC is characterized by strong invasiveness, limited therapeutic opportunities, and adverse prognosis. The 3-year survival rate of HCC is 12.7%, and a median survival is 9 months[1,3]. Only 30%–40% of HCC patients are diagnosed at an early stage and have opportunities for potentially curative treatments[2,4]. Considering the complexity of early evaluation and treatment of HCC, further understanding of the regulation mechanisms and upstream signal moleculars underlying HCC progression is of importance for early diagnosis and treatment.

MafF is a member of the basic leucine zipper (bZIP) transcription factor Maf (muscoloaponeurotic fibrosarcoma oncogene) family. Similar to the other two small Maf proteins (MafG and MafK), MafF lacks an obvious transactivation domain but can homodimerize with small Mafs or heterodimerize with other bZIP proteins, such as the Cap'n'Collar (CNC) family members p45 NFE2, Nrf1, and Nrf2[5,6]. Through the homodimers or heterodimers that function as transcriptional repressors or activators, MafF plays important roles in the control of gene expression and participates in a variety of physiological and pathological processes such as hematopoiesis, cellular stress response, and cancer development[7–9].

In previous studies, MafF has been associated with liver development and diseases. The triple knockout mice of small Mafs (MafF/G/K) showed fetal liver hypoplasia and embryonic lethality[10]. MafF expression increased rapidly during liver regeneration after partial hepatectomy in rats[11]. MafF was also significantly increased in murine liver during development of diet-induced obesity[12]. Comprehensive analysis comprising 1,975 published

[1]These authors provided equal contribution to this work.
Address correspondence to Xiaoxia Ye, Department of Histology and Embryology, Guangdong Medical University, No. 2 Wenming Dong Road, Zhanjiang, Guangdong 524023, P.R. China. Tel: +86-759-2388-575; E-mail: yexx@gdmu.edu.cn

microarrays using the Genomica software package found that the expression of MafF in multiple human tumors was decreased, including HCC[13]. Antioxidant response element (ARE) activators pyrrolidinedithiocarbamate (PDTC) and phenylethyl isothiocyanate (PEITC) could induce MafF expression in HCC cells[14]. A recent study reported that MafF could affect invasion of HCC via regulating the expression of tumor suppressor TFPI2 in retinoid-treated HCC cells[15]. These researches indicated that MafF was closely related to liver development, metabolism, and HCC.

Small noncoding RNAs, including microRNAs (miRNAs) and circular RNAs (circRNAs), can regulate the expression of target genes posttranscriptionally. miRNAs are endogenous small noncoding RNAs, which can induce translational repression and mRNA decay through binding to recognition sequences in the 3′-untranslated region (3′-UTR) of target mRNAs[16,17]. CircRNAs, a novel class of endogenous noncoding RNAs, are characterized as covalently closed loop structures with neither a 5′ cap nor a 3′ polyadenylated tail[18]. The critical functions of circRNAs include miRNA sponges, protein-coding potential, and transcription regulation[19,20]. Growing evidence had shown that the dysregulation of circRNAs contributed to tumorigenesis and progression including HCC[21]. For example, circTRIM33-12 could upregulate the ten eleven translocation 1 (TET1) expression and suppress HCC progression by sponging miR-191[22].

Up to now, the influence of MafF expression on HCC remains unclear. More importantly, to the best of our knowledge, whether noncoding RNAs can regulate MafF expression is completely unexplored. In the current study, we investigated the relationship between MafF expression and HCC progression and explored the noncoding RNA-dependent regulatory mechanism of MafF expression in HCC cells. Our study revealed that MafF acted as a tumor suppressor in HCC, and its expression could be regulated by the circ-ITCH/miR-224-5p axis. This work gives a better understanding of MafF in HCC, which may be helpful for the diagnosis and treatment of HCC in the future.

MATERIALS AND METHODS

Patients and Tissue Samples

A total of 76 paired HCC tumor tissues and adjacent hepatic tissues were collected from the Affiliated Hospital of Guangdong Medical University (Zhanjiang, China) between 2015 and 2017. The patients comprised 50 men and 26 women with an average age of 56.2 years (range: 20–77). The patients had not received any radiotherapy or chemotherapy before operation. All samples were confirmed by pathological diagnosis. The clinical stage of patients was classified according to the pathology tumor–node–metastasis (pTNM) system issued by the American Joint Committee on Cancer/Union for International Cancer Control in 2010. Fresh tissues were snap frozen in liquid nitrogen and stored at −80°C. All patients enrolled in this study signed the informed consent documents. The procedure of the present study was approved by the Medical Ethic Committee of the hospital.

Immunohistochemistry

Immunohistochemical analyses for MafF protein were performed using Polink-2 Plus Detection Kit (ZSGB-BIO, Beijing, China) in 76 paired HCC and adjacent samples. The paraffin-embedded tissue sections were deparaffinized with xylene and rehydrated with graded ethanol. For antigen retrieval, sections were immersed in 10 mM citrate buffer and microwaved for 5 min. Endogenous peroxidase and nonspecific protein binding were blocked by incubating with 3% H_2O_2 and then with 10% goat serum. Next, sections were incubated with the rabbit anti-MafF primary antibody (dilution 1:50; ab110824; Abcam, Cambridge, UK) at 4°C overnight, followed by incubation with the polymer helper for 15 min and then with horseradish peroxidase (HRP) polymer anti-rabbit IgG for 15 min. Finally, signals were visualized with 3,3-diaminobenzidine (DAB) substrate for 1 min and slightly counterstained with hematoxylin. In each experiment, the primary antibody was omitted as a negative control. The sections were evaluated independently by two investigators evaluated independently according to our previous report with slight modification[23]. The degree of immunohistochemical staining was assessed by multiplying the staining intensity score (0: no, 1: light yellow, 2: yellow, and 3: brown yellow) and the staining proportion score (0: < 25%, 1: 25%–50%, 2: 51%–75%, and 3: >75%). The sections with a final score of ≥3 were defined as positive; otherwise, they were defined as negative.

Cell Culture

Human normal hepatic cell line L-O2 and three human HCC cell lines (SMMC7721, Huh7, and Hep3B) were purchased from the Type Culture Collection of the Chinese Academy of Sciences (Shanghai, China). L-O2 cells were cultivated in RPMI-1640 (GIBCO, Grand Island, NY, USA) medium supplemented with 20% fetal bovine serum (FBS) (GIBCO). HCC cells were cultivated in Dulbecco's modified Eagle's medium (DMEM; GIBCO) containing 10% FBS. All cells were grown in a humidified incubator with 5% CO_2 at 37°C.

Lentivirus Infection and Cell Transfection

The 495-base pair (bp) fragment of MafF full-length coding cDNA sequence was amplified from pCMV-Myc-MafF plasmid stored in our lab and then cloned into the lentivirus vector pLVX-mcherry-N1. The 873-bp fragment of cDNA containing exon 6 to exon 12 of the ITCH gene

was amplified from cDNA of 293T cells and then cloned into lentivirus vector pLCDH-cir (RiboBio, Guangzhou, China). The sequences of all constructs were confirmed by DNA sequencing (BGI-Tech, Shenzhen, China). Lentiviral packing and infection of SMMC7721 and Hep3B cells were performed by FITGENE (Guangzhou, China). The cells stably overexpressing MafF or circ-ITCH were established by 1.0% puromycin selection for 1 week and maintained in 0.5% puromycin. Empty vectors were used as negative controls.

miR-224-5p mimics, miR-760 mimics, and mimics control (miR-NC) were purchased from RiboBio. A total of 2×10^5 cells were plated in six-well plates. After 12 h, cells were transfected with miRNA mimics or miR-NC using Lipofectamine 3000 (Thermo Fisher Scientific, Waltham, MA, USA) according to the manufacturer's instructions.

Cell Counting Kit-8 (CCK8) Assay

The MafF or circ-ITCH stably overexpressing or control cells were seeded in 96-well plates at a density of 5,000 cells per well. Circ-ITCH overexpressing and control cells (circ-vector) were transfected with miRNA mimics or miR-NC after seeding for 12 h. At 24, 48, 72, and 96 h after seeding, cell viability was measured by CCK-8 (Beyotime, Shanghai, China) according to the manufacturer's instructions. Briefly, each well was added with 10 μl of CCK-8 solutions, and the plate was incubated at 37°C for 1 h in darkness. Absorbance at 450 nm of each well was measured using a microplate reader (Infinite M200 Pro; TECAN, Männedorf, Switzerland). Three independent experiments were performed with five replicates in each experiment.

Colony Formation Assay

After digestion, cells were counted by an automated cell counter (Scepter, Millipore, Billerica, MA, USA). A total of 300 cells were seeded into six-well plates. Cell transfection treatment was in line with the CCK-8 assay. After 2 weeks of incubation, the cells were fixed with methanol and stained with 0.1% crystal violet. Then the number of cell colonies (>50 cells) was counted. Three independent experiments were performed.

Cell Apoptosis Assay

Cells were seeded in six-well plates at a density of 1×10^6 cells per well. Twelve hours later, circ-ITCH-overexpressing or circ-vector cells were transfected with miRNA mimics or miR-NC. After seeding for 48 h, all cells were collected and stained with Annexin-V–fluorescein isothiocyanate (FITC)/propidium iodide (PI) apoptosis assay kit (Yeasen, Shanghai, China), and then analyzed using a flow cytometry (Epics XL-MCL; Beckman Coulter, Brea, CA, USA). The experiments were repeated three times.

Dual-Luciferase Assay

The dual-luciferase assay was conducted as previously reported[24]. Briefly, 40,000 cells of SMMC7721 or Hep3B were cultivated in 24-well plates and incubated for 12 h before transfection. The pGL3-MafF-3′-UTR-wild type (WT) plasmid or pGL3-MafF-3′-UTR-mutant (Mut1 or Mut2) plasmid was constructed and then was cotransfected with pRL-TK plasmid (Promega, Madison, WI, USA) and miR-224-5p/miR-760 mimics or miR-NC using Lipofectamine 3000 (Thermo Fisher Scientific). After transfection for 48 h, the cells were harvested and the firefly and *Renilla* luciferase activities were determined by dual-luciferase assay kit (Promega). Finally, ratios of luminescence were calculated. Each assay was repeated in three independent experiments.

RNA Extraction and Quantative Real-Time Polymerase Chain Reaction (qRT-PCR)

Total RNA was isolated from tissues and cells using TRIzol reagent (Invitrogen, Carlsbad, CA, USA), and RNA purity was evaluated based on the A260/A280 ratio. The cDNAs were synthesized using the PrimeScript RT Reagent Kit (Takara, Dalian, China). qRT-PCR for MafF mRNA, miRNA, and circRNA was performed using SYBR Premix ExTaq II kit (Takara) through an ABI7500 thermorecycler (Applied Biosystems, Foster City, CA, USA). The primers were synthesized by BGI-Tech (Shenzhen, China) and are listed in Table 1. The expression of MafF mRNA or circ-ITCH was normalized to β-actin, while expression of miRNAs was normalized

Table 1. List of Primers for qRT-PCR

Name	Forward Primer (5′-3′)	Reverse Primer (5′-3′)
MafF	ATCCCCTATCCAGCAAAGCTC	TTGAGCCGTGTCACCTCCTC
β-Actin	TGACGTGGACATCCGCAAAG	CTGGAAGGTGGACAGCGAGG
miR-224-5p	ACACTCCAGCTGGGTCAAGTCACTAGTGGTTCC	TGGTGTCGTGGAGTCG
miR-760	ACACTCCAGCTGGGCGGCTCTGGGTCTG	TGGTGTCGTGGAGTCG
U6	GCTTCGGCAGCACATATACTAAAT	CGCTTCACGAATTTGCGTCTCAT
circ-ITCH	AGCAATGCAGCAGTTT	TGTAGCCCATCAAGACA

to U6. Each sample was replicated three times, and data were calculated by the 2−ΔΔCt method.

RNA Pull-Down Assay

A biotinylated probe was specifically designed to bind to the junction area of circ-ITCH. The circ-ITCH probe (5′-ACAACTACTTCTTCAACCCATCCAGGT GGCAA-3′) and a control probe (5′-TGTCTGCAATAT CCAGGGTTTCCGATGGCACC-3′) were synthesized by BGI-Tech (Shenzhen, China). Probe-coated beads were prepared by incubating biotinylated circ-ITCH probe or control probe with streptavidin C1 magnetic beads (Life Technologies, Carlsbad, CA, USA) at 25°C for 4 h. About 1×10^7 cells were collected, lysed, and sonicated, and then incubated with probe-coated beads at 4°C overnight. The miRNAs were pulled down by incubating the cell lysates with beads. The beads were washed with washing buffer, and the RNA complexes bound to the beads were eluted and extracted using RNeasy Mini Kit (QIAGEN, Hilden, Germany) for qRT-PCR analysis.

Antibodies and Western Blot

Cells were harvested and lysed with radioimmunoprecipitation assay (RIPA) buffer (Beyotime). Protein extractions were separated by 12% sodium dodecyl sulphate-polyacrylamide gel electrophoresis (SDS-PAGE) and transferred to polyvinylidene fluoride membranes. After 5% nonfat milk blocking, the membranes were incubated with primary antibody at 4°C overnight, followed by incubation with secondary antibody at room temperature for 1 h. After washing, signals were detected using Enhanced ChemiLuminescence detection system (Thermo Fisher Scientific). β-Actin was used as internal control. All antibodies were purchased from Abcam: rabbit anti-MafF primary antibody (cat. ab183859; dilution 1:1,000; 18 kDa), rabbit anti-β-actin primary antibody (cat. ab227387; dilution 1:5,000; 42 kDa), and goat anti-rabbit HRP-labelled IgG (cat. ab205718; dilution 1:10,000).

Statistical Analysis

Data were analyzed with SPSS 17.0 software. Unless otherwise noted, data are presented as mean ± standard deviation (SD) of three independent experiments. The chi-square test was used to analyze the relationship between MafF protein expression and patients' clinical features. Differences between two groups were compared using the Student's *t*-test. Differences between three or more groups were compared with the one-way analysis of variance (ANOVA) test, and least significant difference (LSD) method was used for comparison between groups. The Pearson's correlation analysis was conducted to analyze the correlations. A value of $p < 0.05$ was considered statistically significant.

RESULTS

MafF Expression Was Decreased in HCC Tissues and Cells

To explore the role of MafF in HCC, we firstly detect MafF protein expression in 76 paired HCC and paratumor tissues by immunohistochemistry. As shown in Figure 1A, MafF protein mainly distributed in the nucleus, and its expression level in HCC tissues was lower than that in paratumor tissues. Furthermore, MafF expression decreased with the progression of HCC (Fig. 1B). Next, we examined the expression of MafF protein in human normal hepatic cells L-O2 and three human HCC cell lines SMMC7721, Huh7, and Hep3B. Western blot results showed that the expression of MafF protein was lower in HCC cells than in L-O2 cells (Fig. 1C). Furthermore, we analyzed the correlation between MafF protein level and clinicopathological features of 76 HCC patients (Table 2). We found that MafF protein level was negatively related to HCC pT staging ($p = 0.027$) and pTNM staging ($p = 0.002$), while it had no significant correlationship with other features such as age and tumor size.

MafF Overexpression Inhibited Proliferation and Induced Apoptosis of HCC Cells

Considering that MafF was downregulated in HCC, we further investigated its function by overexpressing MafF in HCC cells. We firstly constructed MafF-overexpressing SMMC7721 and Hep3B cell lines by lentivirus infection followed by puromycin selection. qRT-PCR and Western blot results demonstrated that MafF mRNA and protein levels were significantly elevated in both cells (Fig. 2A and B). CCK-8 assays revealed that MafF overexpression inhibited cell proliferation (Fig. 2C and D). The colony numbers of MafF-overexpressing cells were significantly less than control cells (Fig. 2E and F). Flow cytometry analysis was carried out to evaluate whether MafF affects HCC cell apoptosis. We found that MafF overexpression dramatically increased the apoptosis rate of SMMC7721 and Hep3B cells (Fig. 3). These data indicated that MafF overexpression could inhibit proliferation and induce apoptosis of HCC cells.

MafF Could Be Downregulated by miR-224-5p in HCC Cells

miRNAs can influence mRNA stability or mRNA translation, mainly by binging to 3′-UTR of specific mRNA. We firstly used four miRNA target prediction tools (miRanda, Targetscan, miRWalk, and starBase) to investigate the possible miRNAs that have the potential to bind with MafF mRNA. Two miRNAs, miR-224-5p and miR-760, were found to be the overlap of four databases and were chosen for further study (Fig. 4A and B). After miRNA mimic transfection, the expression

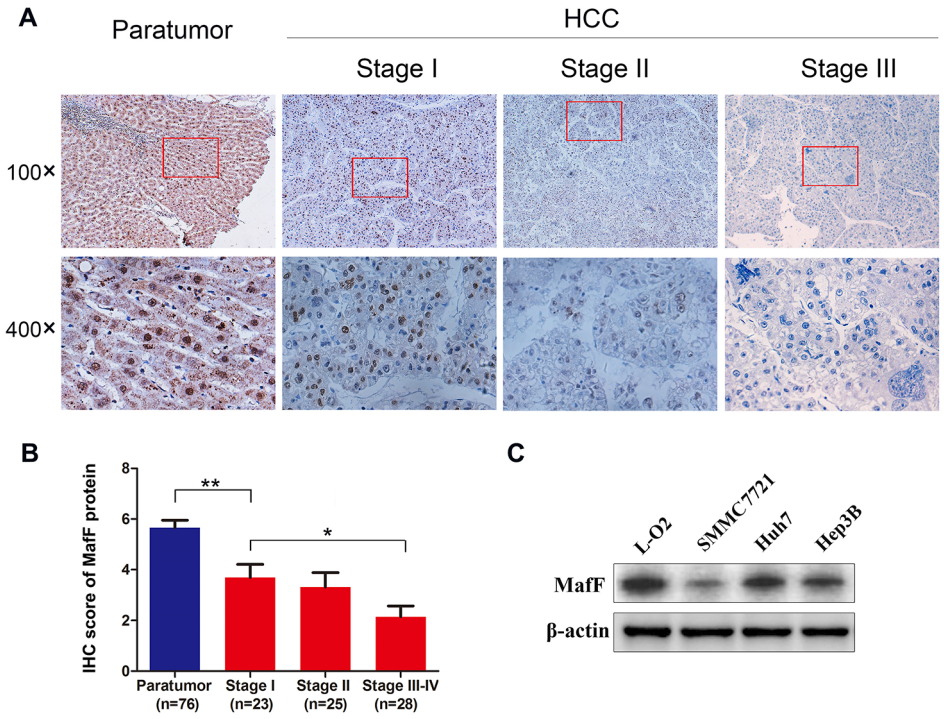

Figure 1. MafF protein expression in hepatocellular carcinoma (HCC) tissues and cell lines. (A) Representative immunohistochemical staining images in paratumor hepatic tissues and different stages of HCC tissues. (B) Comparison of MafF immunohistochemistry (IHC) score between paratumor tissues and HCC tissues of different clinical stages. (C) Expression of MafF protein in L-O2 cell and three HCC cell lines. *$p < 0.05$, **$p < 0.01$ versus paratumor tissues.

Table 2. Relationship Between MafF Protein Expression and Clinicopathological Features of Hepatocellular Carcinoma (HCC) Patients ($N = 76$)

		MafF Expression [*n* (%)]			
Variables	*n*	Negative	Positive	χ^2	*p* Value
Gender				2.155	0.142
Male	50	30 (60.0%)	20 (40.0%)		
Female	26	11 (42.3%)	15 (57.7%)		
Age				0.071	0.790
<55 years	36	20 (55.6%)	16 (44.4%)		
≥55 years	40	21 (52.5%)	19 (47.5%)		
Size				1.033	0.310
<5 cm	52	26 (50%)	26 (50%)		
≥5 cm	24	15 (62.5%)	9 (37.5%)		
pT stage				4.887	0.027*
pT1–2	51	23 (45.1%)	28 (54.9%)		
pT3–4	25	18 (72.0%)	7 (28.0%)		
pN stage				2.683	0.101
pN0	68	34 (50.0%)	34 (50.0%)		
pN1	8	7 (87.5%)	1 (12.5%)		
pM stage				2.800	0.094
pM0	71	36 (50.7%)	35 (49.3%)		
pM1	5	5 (100.0%)	0 (0.0%)		
pTNM				10.014	0.002**
I	23	7 (30.4%)	16 (69.6%)		
II	25	13 (52.0%)	12 (48.0%)		
III–IV	28	21 (75.0%)	7 (25.0%)		

*$p < 0.05$, **$p < 0.01$.

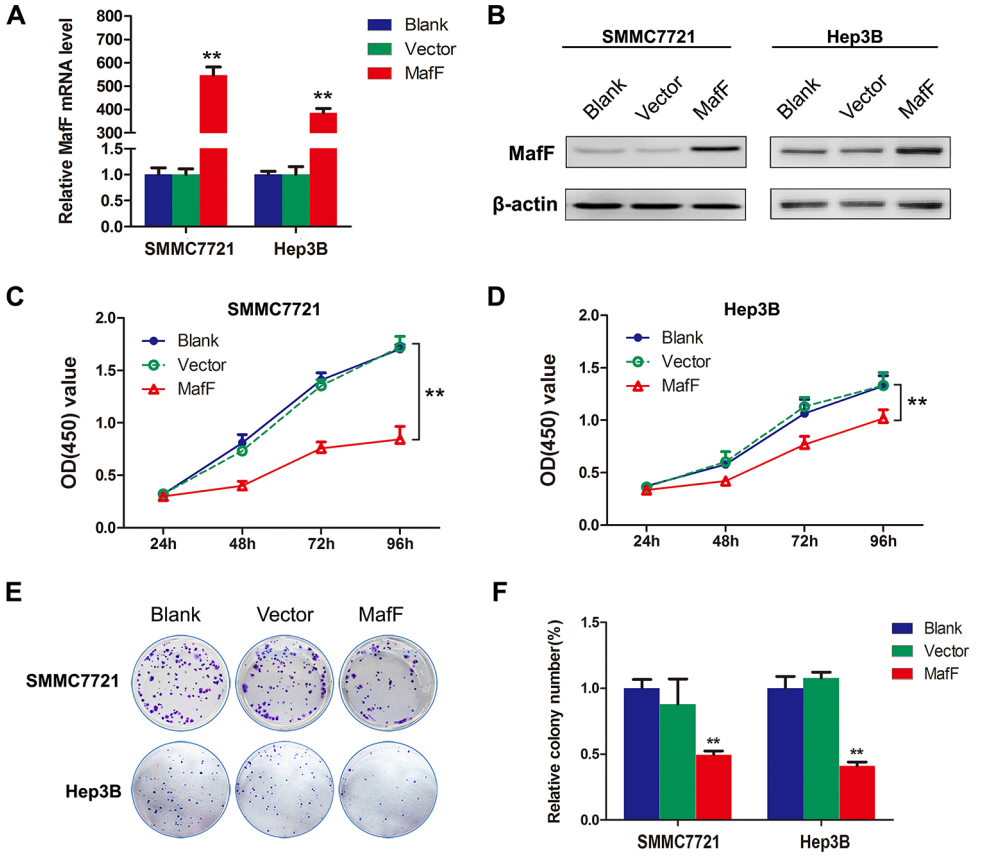

Figure 2. Cell proliferation and colony formation assays. MafF mRNA and protein levels in control cells and MafF-overexpressing cells were detected by quantative real-time polymerase chain reaction (qRT-PCR) (A) and Western blot (B). Cell counting kit-8 (CCK-8) assay was used to evaluate the proliferation capacity of SMMC7721 (C) and Hep3B (D) cells. The OD450 value was measured at 24, 48, 72, and 96 h after cells were seeded. (E, F) The colony numbers of various cell groups were calculated after cultivated for 2 weeks. Three independent experiments were performed. $^{**}p < 0.01$ versus blank or vector group.

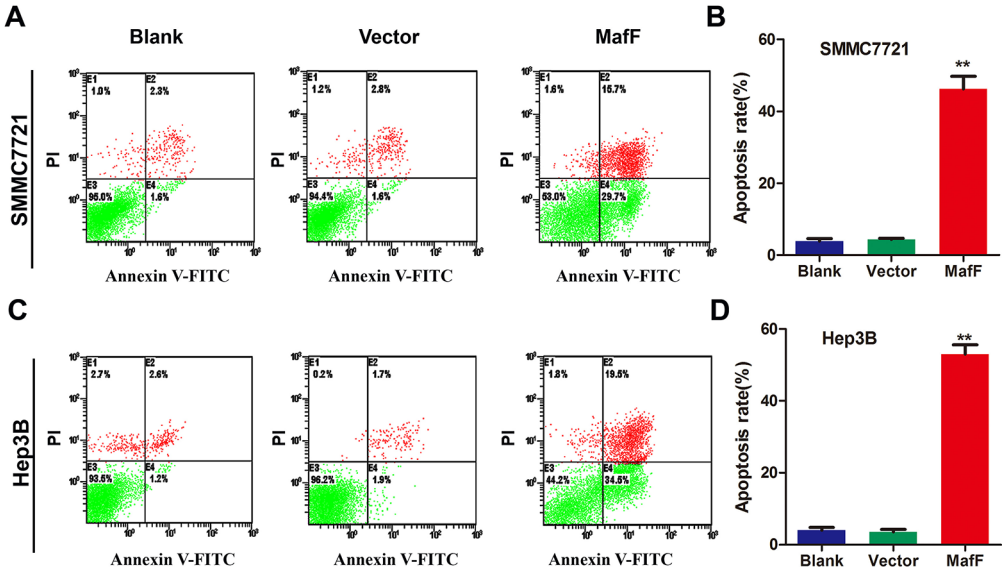

Figure 3. Cell apoptosis assays. Apoptosis rates of control cells or MafF-overexpressing cells were detected by annexin V–fluorescein isothiocyanate (FITC)/propidium iodide (PI) double staining. Representative flow cytometry images in SMMC7721 (A) and Hep3B (C) cells are shown. Apoptosis rates of different cell groups were compared (B and D). Three independent experiments were performed. $^{**}p < 0.01$.

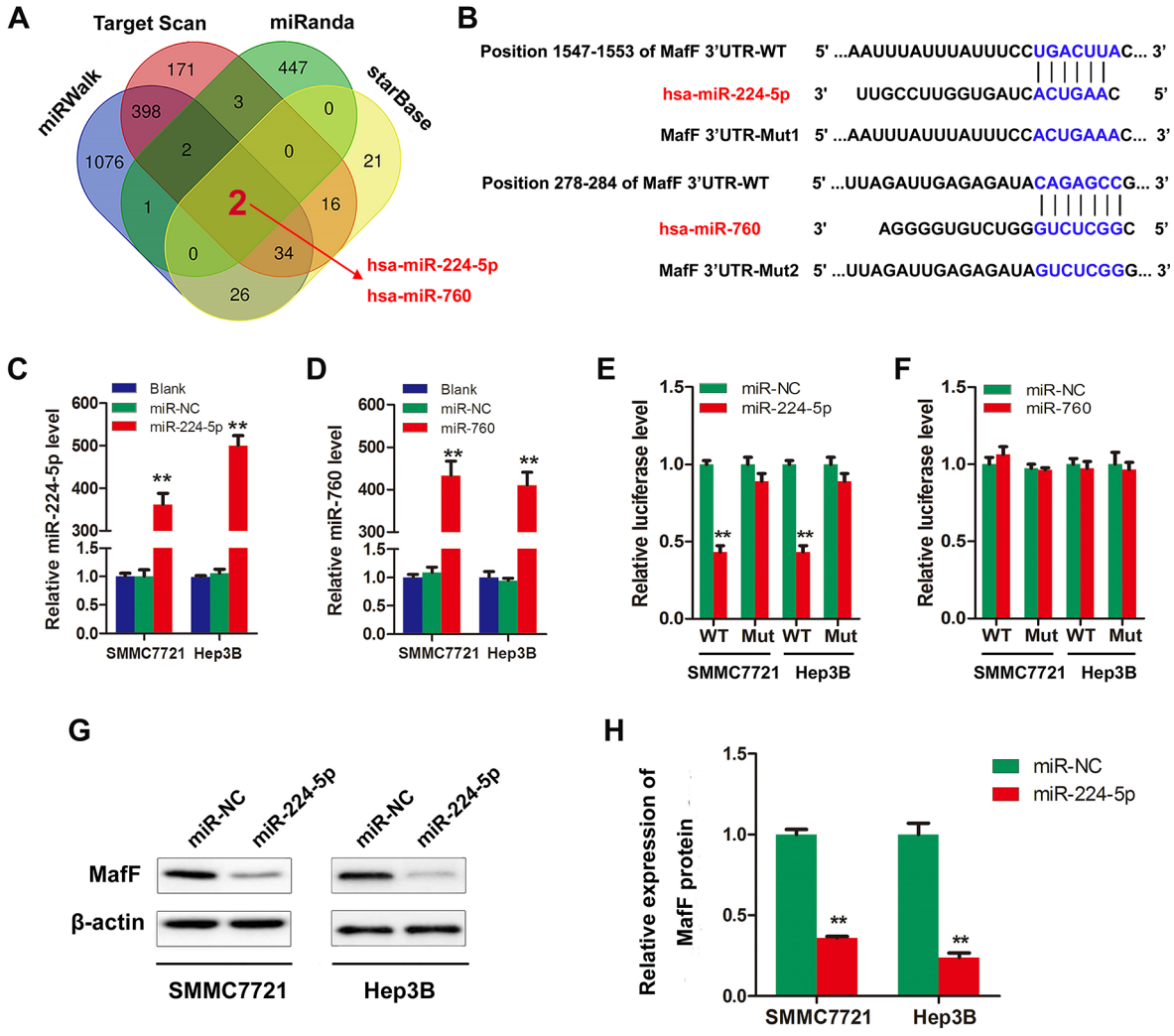

Figure 4. miR-224-5p targeted MafF mRNA and regulated MafF expression in HCC cells. (A) Four miRNA target prediction tools were used to investigate miRNAs that have the potential to bind with MafF mRNA. (B) Binding sites between the 3′-untranslated region (3′-UTR) of MafF and miR-224-5p or miR-760. (C, D) After microRNA (miRNA) mimic transfection, the expression of miR-224-5p and miR-760 was detected by qRT-PCR. (E, F) The dual-luciferase assay was performed after cotransfection with MafF 3′-UTR [wild type (WT) or mutant (Mut)] and miR-224-5p or miR-760 or miR-NC. The firefly luciferase activities were detected, and *Renilla* luciferase activities were used for normalization. (G, H) The MafF protein level was evaluated by Western blot after miR-224-5p mimic or miR-NC transfection. Three independent experiments were performed. $^{**}p < 0.01$.

of mir-224-5p or miR-760 increased greatly (Fig. 4C and D). The luciferase activities were inhibited when cells were cotransfected with miR-224-5p mimics and MafF 3′-UTR-WT compared with those of control miRNA (miR-NC) transfection group. No differences in luciferase activity were found when MafF 3′-UTR-Mut was cotransfected with miR-224-5p or miR-NC. However, miR-760 mimic transfection did not influence the luciferase activity of all group cells (Fig. 4E and F). These results indicated that miR-224-5p could target MafF mRNA directly, but miR-760 could not. Western blot analysis further confirmed that miR-224-5p markedly downregulated MafF protein expression (Fig. 4G and H). Taken together, our experiments confirmed that miR-224-5p directly targeted MafF mRNA and decreased the protein level of MafF.

CircRNA circ-ITCH Was a Molecular Sponge of miR-224-5p in HCC

Previous studies have reported that circ-ITCH functioned as a miR-224-5p sponge and subsequently abolished the oncogenic effect of miR-224-5p in bladder cancer[25]. In order to investigate whether circ-ITCH can affect HCC progress by sponging miR-224-5p, we first detected the expression of circ-ITCH and miR-224-5p in HCC. qRT-PCR results showed that circ-ITCH levels

were downregulated in HCC compared with paratumor tissues and decreased with the progression of HCC (Fig. 5A), which was consistent with the expression pattern of MafF. Then we detected levels of circ-ITCH and miR-224-5p in L-O2 and three HCC cell lines. Compared with L-O2 cells, HCC cells showed lower circ-ITCH levels and higher miR-224-5p levels (Fig. 5B). Subsequent correlation analysis revealed that circ-ITCH level was negatively related to miR-224-5p level ($r = -0.453$, $p = 0.000$) in HCC tissues (Fig. 5C). RNA pull-down assay showed an obvious enrichment of miR-224-5p in the circ-ITCH probe pellet compared with the control probe pellet. These results demonstrated that circ-ITCH could directly bind and sponge miR-224-5p (Fig. 5D).

Circ-ITCH/miR-224-5p Axis Regulated Cell Proliferation and Apoptosis by Modulating MafF Expression

Based on the results that circ-ITCH could sponge miR-224-5p, and miR-224-5p could target MafF mRNA to suppress its expression, we speculated that the tumor-suppressive effects of MafF may be regulated by the circ-ITCH/miR-224-5p axis. To verify the speculation, circ-ITCH overexpression cells were constructed by lentivirus infection. We found that enforced expression of circ-ITCH significantly upregulated the MafF protein level (Fig. 6A–F), promoted cell proliferation (Fig. 6G), and induced cell apoptosis (Fig. 6H). Subsequent rescue experiment results showed that miR-224-5p transfection reversed the upregulation of MafF protein induced by circ-ITCH (Fig. 6B, C, E, and F), and partly counteracted the antiproliferation and proapoptosis effects of circ-ITCH (Fig. 6G, H, and I). Collectively, these data reflected that decreased expression of MafF in HCC could be modulated via the circ-ITCH/miR-224-5p axis and consequently promoted tumor progression (Fig. 6J).

DISCUSSION

In this study, we found that MafF was downregulated in HCC tissues and cells and decreased with the progression of HCC clinical stage. Overexpression of MafF could inhibit the proliferation and colony formation and induce apoptosis of HCC cells. These results suggested that MafF acted as a tumor suppressor, and its expression was associated with HCC progression. On the basis of these results, we further explored the regulation mechanism of MafF in HCC.

It is well known that miRNAs can regulate numerous genes posttranscriptionally, but whether MafF can be regulated by miRNAs is still unclear. We therefore investigated miRNAs that could bind to MafF mRNA

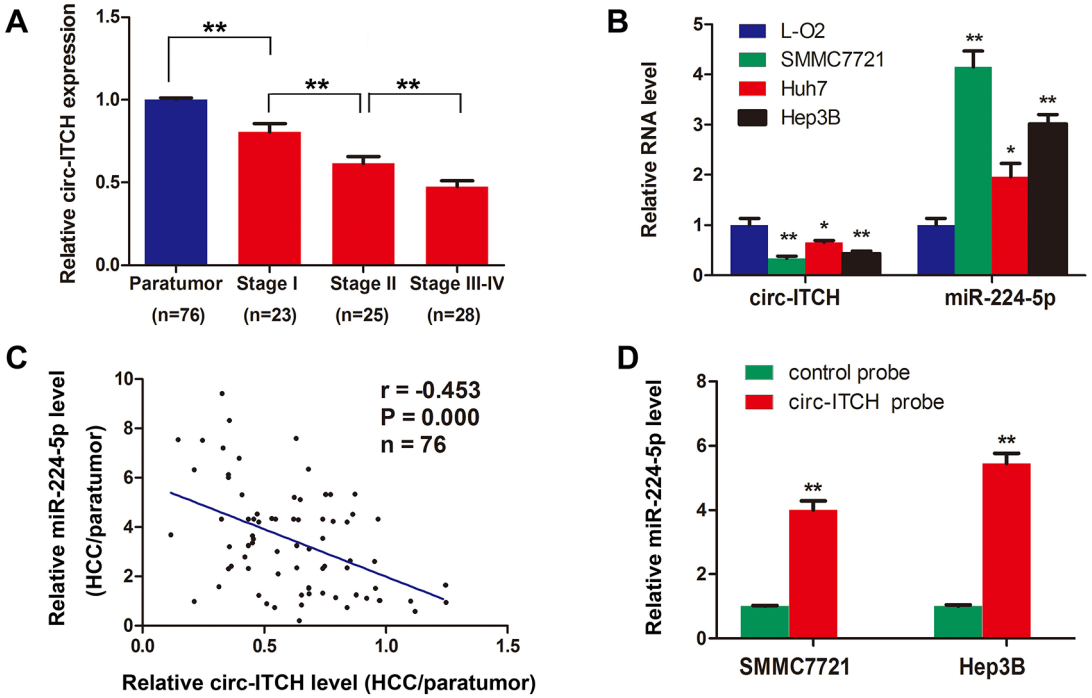

Figure 5. Circ-ITCH was decreased and could sponge miR-224-5p in HCC. (A) Expression of circ-ITCH in HCC and adjacent normal tissues was detected by qRT-PCR. (B) Expression of circ-ITCH and miR-224-5p in L-O2 and HCC cells was detected by qRT-PCR. (C) Expression of circ-ITCH and miR-224-5p in 76 paired HCC and adjacent normal tissues was detected by qRT-PCR, and their correlationship was evaluated by Person's correlation analysis. (D) miR-224-5p was pulled down and enriched by biotin-coupled circ-ITCH specific probe, and then detected by qRT-PCR. *$p < 0.05$, **$p < 0.01$.

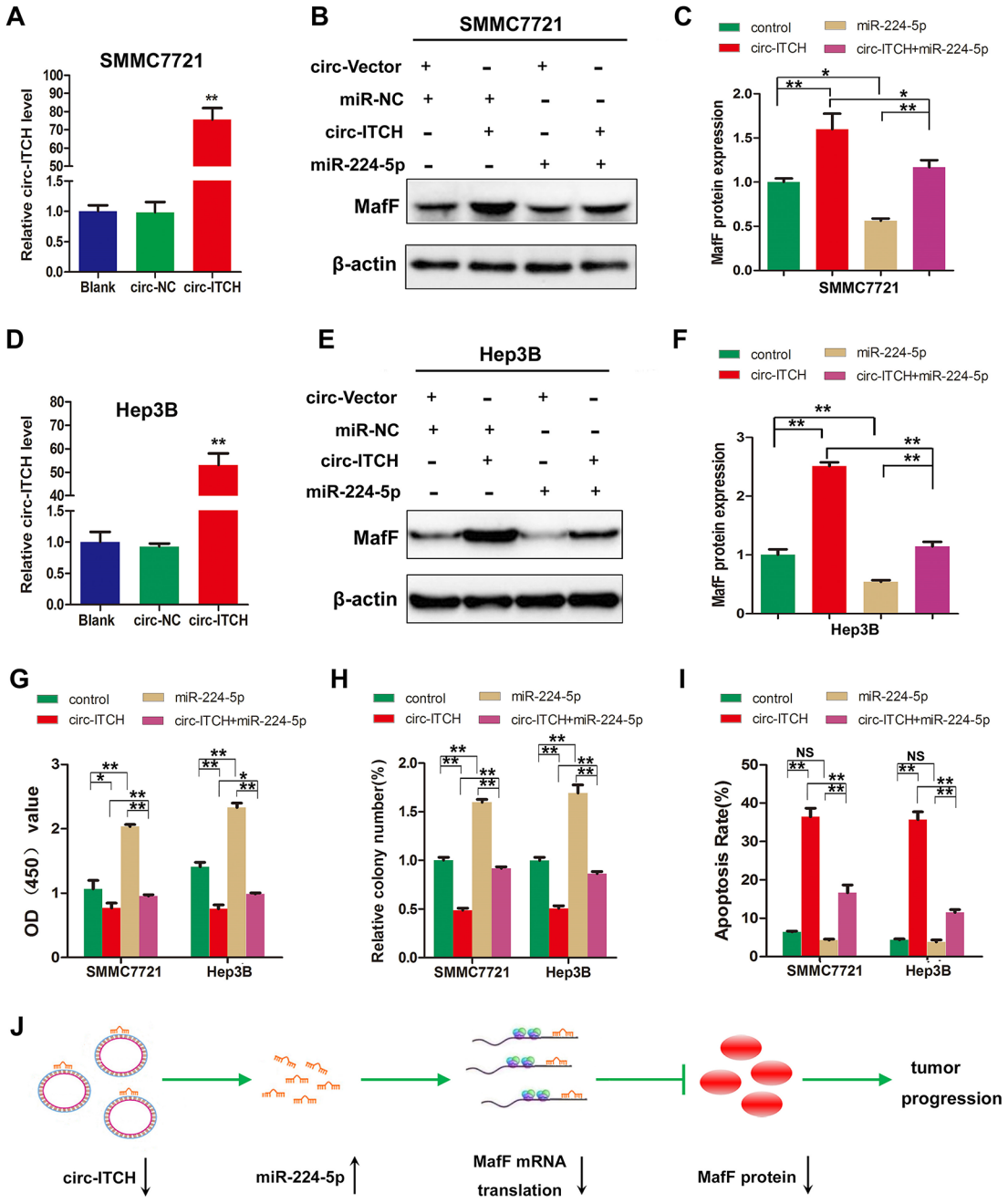

Figure 6. The expression and antitumor effects of MafF could be regulated via the circ-ITCH/miR-224-5p axis. (A, D) Circ-ITCH was overexpressed by lentivirus infection in SMMC7721 and Hep3B cells. Protein expression of MafF in SMMC7721 cells (B, C) and Hep3B cells (E, F) was detected by Western blot after transfection of miR-224-5p mimics or miR-NC. (G, H) The cell viability was measured by CCK-8 assay and colony formation assay after tranfection. (I) The cell apoptosis was detected by annexin V–FITC/PI double staining. (J) Schematic of the current study. $*p < 0.05$, $**p < 0.01$.

by bioinformatics analysis, and two candidate miRNAs were screened out. Subsequent experiments confirmed that miR-224-5p could directly bind to the 3′-UTR of MafF and downregulate MafF expression. miR-224-5p is frequently dysregulated in multiple cancers and acts as an oncogenic miRNA by targeting tumor suppressor genes such as p21 and Smad4[26]. In HCC, it is highly upregulated and promises to be a valuable early diagnostic biomarker[27,28]. Recently, it was reported that miR-224-5p directly targeted glycine N-methyltransferase (GNMT) to promote tumorigenesis of HCC[29]. Our present study identified MafF as a novel target gene of miR-224-5p in

HCC. Moreover, the antitumor effects of MafF could be regulated by miR-224-5p.

CircRNAs commonly act as miRNA sponges and repress miRNA activities[30]. Recently, a study reported that circ-ITCH could inhibit bladder cancer progression by sponging miR-224[25]. Circ-ITCH is regarded as a tumor suppressor and is downregulated in various cancers, including ovarian cancer[31], lung cancer[32], and osteosarcoma[33]. In HCC, the expression of circ-ITCH decreased in tumor tissues, and its low expression was associated with poor survival of HCC[34], but the related molecular pathway was still unexplored. In the present study, we verified that circ-ITCH was downregulated in HCC tissues and cells. Mechanistically, we found that circ-ITCH could directly sponge miR-224-5p to upregulate the expression of MafF in HCC. The rescue experiments elucidated that the antitumor effects of MafF could be modulated via the circ-ITCH/miR-224-5p axis.

In summary, our study was the first to explore the role of MafF in HCC and disclosed a novel circ-ITCH/miR-224-5p/MafF regulation pathway. Low MafF expression induced by this dysegulated pathway in HCC could promote cell proliferation and tumor progression. But the downstream signal moleculars of this pathway in HCC are still unclear. Previous researches indicated that MafF participated in oxidant stress response, inflammatory response, and cell motility by regulating the transcription of related genes such as heme oxygenase 1 (HO-1) and matrix metalloproteinases (MMPs)[9,35]. More studies need to be performed to elucidate the exact downstream moleculars of the circ-ITCH/miR-224-5p/MafF pathway in HCC, which will provide a new perspective for early diagnostic biomarkers and potential therapeutic targets of HCC.

ACKNOWLEDGMENTS: This research was funded by the Natural Science Foundation of Guangdong Province (2018A030310106, 2018 A030310116, and 2019A1515012007), Administration of Traditional Chinese Medicine of Guangdong Province (A20171148), Science and Technology Project of Zhanjiang (2019B01023), and Special Fund for Group-Type Assistance of Education Talents in Colleges and Universities of Guangdong Province (4SG19047G). The authors declare no conflicts of interest.

REFERENCES

1. Ferlay J, Soerjomataram I, Dikshit R, Eser S, Mathers C, Rebelo M, Parkin DM, Forman D, Bray F. Cancer incidence and mortality worldwide: Sources, methods and major patterns in GLOBOCAN 2012. Int J Cancer 2015;136(5):E359–86.
2. Yarchoan M, Agarwal P, Villanueva A, Rao S, Dawson LA, Llovet JM, Finn RS, Groopman JD, El-Serag HB, Monga SP, Wang XW, Karin M, Schwartz, RE, Tanabe KK, Roberts LR, Gunaratne PH, Tsung A, Brown KA, Lawrence TS, Salem R, Singal AG, Kim AK, Rabiee A, Resar L, Hoshida Y, He AR, Ghoshal K, Ryan PB, Jaffee EM, Guha C, Mishra L, Coleman CN, Ahmed MM. Recent developments and therapeutic strategies against hepatocellular carcinoma. Cancer Res. 2019;79(17):4326–30.
3. Giannini EG, Farinati F, Ciccarese F, Pecorelli A, Rapaccini GL, Di Marco M, Benvegnu L, Caturelli E, Zoli M, Borzio F, Chiaramonte M, Trevisani F. Prognosis of untreated hepatocellular carcinoma. Hepatology 2015;61 (1):184–90.
4. Kim DW, Talati C, Kim R. Hepatocellular carcinoma (HCC): Beyond sorafenib—Chemotherapy. J Gastrointest Oncol. 2017;8(2):256–65.
5. Motohashi H, Katsuoka F, Engel JD, Yamamoto M. Small Maf proteins serve as transcriptional cofactors for keratinocyte differentiation in the Keap1–Nrf2 regulatory pathway. Proc Natl Acad Sci USA 2004;101(17):6379–84.
6. Katsuoka F, Yamamoto M. Small Maf proteins (MafF, MafG, MafK): History, structure and function. Gene 2016;586(2):197–205.
7. Blank V. Small Maf proteins in mammalian gene control: Mere dimerization partners or dynamic transcriptional regulators? J Mol Biol. 2008;376(4):913–25.
8. Kannan MB, Solovieva V, Blank V. The small MAF transcription factors MAFF, MAFG and MAFK: Current knowledge and perspectives. Biochim Biophys Acta 2012;1823(10):1841–6.
9. Saliba J, Coutaud B, Solovieva V, Lu F, Blank V. Regulation of CXCL1 chemokine and CSF3 cytokine levels in myometrial cells by the MAFF transcription factor. J Cell Mol Med. 2019;23(4):2517–25.
10. Yamazaki H, Katsuoka F, Motohashi H, Engel JD, Yamamoto M. Embryonic lethality and fetal liver apoptosis in mice lacking all three small Maf proteins. Mol Cell Biol. 2012;32(4):808–16.
11. Xu CS, Shao HY, Du B. Study on correlation of signal molecule genes and their receptor-associated genes with rat liver regeneration. Genome 2009;52(6):505–23.
12. Kim J, Kwon EY, Park S, Kim JR, Choi SW, Choi MS, Kim SJ. Integrative systems analysis of diet-induced obesity identified a critical transition in the transcriptomes of the murine liver and epididymal white adipose tissue. Int J Obes. (Lond) 2016;40(2):338–45.
13. Amit I, Citri A, Shay T, Lu Y, Katz M, Zhang F, Tarcic G, Siwak D, Lahad J, Jacob-Hirsch J , Amariglio N, Vaisman N, Segal E, Rechavi G, Alon U, Mills GB, Domany E, Yarden Y. A module of negative feedback regulators defines growth factor signaling. Nat Genet. 2007;39 (4):503–12.
14. Moran JA, Dahl EL, Mulcahy RT. Differential induction of mafF, mafG and mafK expression by electrophile-response-element activators. Biochem J. 2002;361(Pt 2):371–7.
15. Tsuchiya H, Oura S. Involvement of MAFB and MAFF in retinoid-mediated suppression of hepatocellular carcinoma invasion. Int J Mol Sci. 2018;19(5):E1450.
16. Iwakawa HO, Tomari Y. The functions of microRNAs: mRNA decay and translational repression. Trends Cell Biol. 2015;25(11):651–65.
17. Jiang C, Liu X, Wang M, Lv G, Wang G. High blood miR-802 is associated with poor prognosis in HCC patients by regulating DNA damage response 1 (REDD1)-mediated function of T cells. Oncol Res. 2019;27(9):1025–34.
18. Zhong Y, Du Y, Yang X, Mo Y, Fan C, Xiong F, Ren D, Ye X, Li C, Wang Y , Wei F, Guo C, Wu X, Li X, Li Y, Li G, Zeng Z, Xiong W. Circular RNAs function as ceRNAs to regulate and control human cancer progression. Mol Cancer 2018;17(1):79.

19. Wang J, Zhu S, Meng N, He Y, Lu R, Yan GR. ncRNA-encoded peptides or proteins and cancer. Mol Ther. 2019;27(10):1718–25.
20. Kristensen LS, Andersen MS, Stagsted LVW, Ebbesen KK, Hansen TB, Kjems J. The biogenesis, biology and characterization of circular RNAs. Nat Rev Genet. 2019;20(11):675–91.
21. Wu J, Qi X, Liu L, Hu X, Liu J, Yang J, Lu L, Zhang Z, Ma S, Li H, Yun X, Sun T, Wang Y, Wang Z, Liu Z, Zhao W. Emerging epigenetic regulation of circular RNAs in human cancer. Mol Ther Nucleic Acids 2019;16:589–96.
22. Zhang PF, Wei CY, Huang XY, Peng R, Yang X, Lu JC, Zhang C, Gao C, Cai JB, Gao PT, Gao DM, Shi GM, Ke AW, Fan J. Circular RNA circTRIM33-12 acts as the sponge of MicroRNA-191 to suppress hepatocellular carcinoma progression. Mol Cancer 2019;18(1):105.
23. Ye X, Mo M, Xu S, Yang Q, Wu M, Zhang J, Chen B, Li J, Zhong Y, Huang Q, Cai C. The hypermethylation of p16 gene exon 1 and exon 2: Potential biomarkers for colorectal cancer and are associated with cancer pathological staging. BMC Cancer 2018;18(1):1023.
24. Wu M, Ye X, Wang S, Li Q, Lai Y, Yi Y. MicroRNA-148b suppresses proliferation, migration, and invasion of nasopharyngeal carcinoma cells by targeting metastasis-associated gene 2. Onco Targets Ther. 2017;10:2815–22.
25. Yang C, Yuan W, Yang X, Li P, Wang J, Han J, Tao J, Yang H, Lv Q, Zhang W. Circular RNA circ-ITCH inhibits bladder cancer progression by sponging miR-17/miR-224 and regulating p21, PTEN expression. Mol Cancer 2018;17(1):19.
26. Chen W, Fan XM, Mao L, Zhang JY, Li J, Wu JZ, Tang JH. MicroRNA-224: As a potential target for miR-based therapy of cancer. Tumour Biol. 2015;36(9):6645–52.
27. Wang Y, Lee CG. Role of miR-224 in hepatocellular carcinoma: A tool for possible therapeutic intervention? Epigenomics 2011;3(2):235–43.
28. Cui Y, Xu HF, Liu MY, Xu YJ, He JC, Zhou Y, Cang SD. Mechanism of exosomal microRNA-224 in development of hepatocellular carcinoma and its diagnostic and prognostic value. World J Gastroenterol. 2019;25(15):1890–8.
29. Hung JH, Li CH, Yeh CH, Huang PC, Fang CC, Chen YF, Lee KJ, Chou CH, Cheng HY, Huang HD, et al. MicroRNA-224 down-regulates glycine *N*-methyltransferase gene expression in hepatocellular carcinoma. Sci Rep. 2018;8(1):12284.
30. Zhou R, Wu Y, Wang W, Su W, Liu Y, Wang Y, Fan C, Li X, Li G, Li Y, Xiong W, Zeng Z. Circular RNAs (circRNAs) in cancer. Cancer Lett. 2018;425:134–42.
31. Luo L, Gao Y, Sun X. Circ-ITCH correlates with small tumor size, decreased FIGO stage and prolonged overall survival, and it inhibits cells proliferation while promotes cells apoptosis in epithelial ovarian cancer. Cancer Biomark. 2018;23(4):505–13.
32. Wan L, Zhang L, Fan K, Cheng ZX, Sun QC, Wang JJ. Circular RNA-ITCH suppresses lung cancer proliferation via inhibiting the Wnt/beta-catenin pathway. Biomed Res Int. 2016;2016:1579490.
33. Ren C, Liu J, Zheng B, Yan P, Sun Y, Yue B. The circular RNA circ-ITCH acts as a tumour suppressor in osteosarcoma via regulating miR-22. Artif Cells Nanomed Biotechnol. 2019;47(1):3359–67.
34. Guo W, Zhang J, Zhang D, Cao S, Li G, Zhang S, Wang Z, Wen P, Yang H, Shi X, Pan J, Ye H. Polymorphisms and expression pattern of circular RNA circ-ITCH contributes to the carcinogenesis of hepatocellular carcinoma. Oncotarget 2017;8(29):48169–77.
35. Massrieh W, Derjuga A, Blank V. Induction of endogenous Nrf2/small maf heterodimers by arsenic-mediated stress in placental choriocarcinoma cells. Antioxid Redox Signal 2006;8(1–2):53–9.